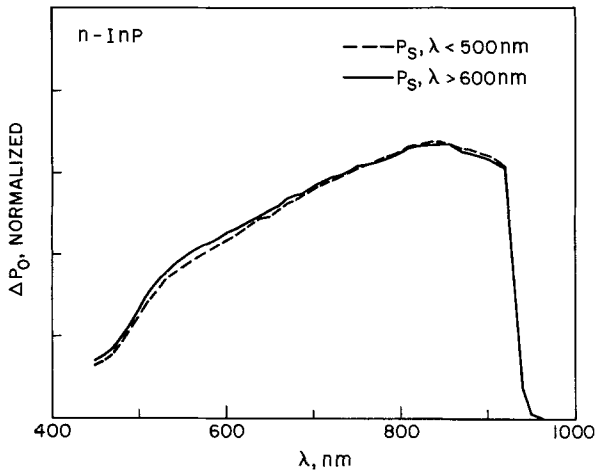

Fig. 9. Modulated power spectra ΔP_0 *vs.* λ of n-InP. The solid line shows the spectra under low energy excitation; the dash line, under high energy excitation.

Thus, the current efficiency for surface oxidation is indicated to be less than a few percent.

Maximum power spectra for n-InP in this system, shown in Fig. 9, were analogous to those for n-CdSe and c-Si, except for the bandgap (1.35 eV). P_s beams with either short or long wavelength photons in equal numbers have no differentiating effect on the ΔP_0 response. All three examples of crystalline semiconductors studied here were thus parallel in this regard. This would be the classical expectation: all photons of greater than bandgap energy produce the same output and thus show no excitation wavelength differentiation.

Conclusions

The recently introduced method of maximum power spectroscopy has been used to characterize amorphous silicon and three n-type crystalline Si, CdSe, and InP semiconductor photoelectrodes. With a superimposed beam of either short or long wavelength excitation, the thin film of a-Si:H was the only material to exhibit a wavelength dependent effect in the differential power output spectrum. However, under the same conditions, the differential short-circuit quantum efficiency spectrum displays no dependence on the wavelength distribution of the steady beam when it is normalized to constant dc cell output.

RRDE studies evidence that n-CdSe and n-InP photoanodes in this methanolic medium operate in a regenerative manner. Photocorrosion and/or photopassivation processes at these electrodes are largely circumvented under these operating conditions. The stability of n-InP is more sensitive to light intensity and electrolyte purity and decreases on extended potential cycling.

Acknowledgment

The authors wish to express their appreciation to N. S. Lewis of Stanford University for generously supplying us with epoxy-mounted a-Si:H photoelectrodes.

Manuscript submitted May 14, 1984; revised manuscript received Sept. 10, 1984.

AT&T Bell Laboratories assisted in meeting the publication costs of this article.

REFERENCES

1. B. Miller and J. M. Rosamilia, *This Journal*, **131,** 2266 (1984).
2. C. M. Gronet, N. S. Lewis, G. W. Cogan, J. F. Gibbon, G. R. Moddel, and H. Weismann, *ibid.*, **131,** 2873 (1984).
3. C. M. Gronet, N. S. Lewis, C. Cogan, and J. Gibbons, *Proc. Nat'l Acad. Sci., USA*, **80,** 1152 (1983).
4. K. D. Legg, A. B. Ellis, J. M. Bolts, and M. S. Wrighton, *ibid.*, **74,** 4116 (1977).
5. D. Laser and A. J. Bard, *J. Phys. Chem.*, **80,** 459 (1976).
6. Y. Avigal, D. Cohen, G. Hodes, J. Manassen, B. Vainas, and R. A. G. Gibson, *This Journal*, **127,** 1209 (1980).
7. G. S. Calabrese, M-S. Lin, J. Dresner, and M. S. Wrighton, *J. Am. Chem. Soc.*, **104,** 2412 (1982).
8. B. Miller, *This Journal*, **127,** 184 (1980).
9. W. J. Albery and S. Bruckenstein, *Trans. Faraday Soc.*, **62,** 1920 (1966).
10. A. Heller, G. P. Schwartz, R. G. Vadimsky, S. Menezes, and B. Miller, *This Journal*, **125,** 1156 (1978).
11. L. F. Schneemeyer and B. Miller, *ibid.*, **129,** 1977 (1982).
12. B. Miller, *J. Electroanal. Chem.*, **168,** 91 (1984).

Polymer Films on Electrodes.

XVI. *In Situ* Ellipsometric Measurements of Polybipyrazine, Polyaniline, and Polyvinylferrocene Films

Clifford M. Carlin, Larry J. Kepley, and Allen J. Bard*

Department of Chemistry, The University of Texas at Austin, Austin, Texas 78712

ABSTRACT

Ellipsometry was used to study the electrodeposition of polymer films formed by oxidation of bipyrazine, polyvinylferrocene, and aniline. For polymeric films of limited thickness displaying good optical characteristics (*i.e.*, high reflectivity, uniform coverage, and homogeneity), the film refractive index and thickness were determined. Nonideal ellipsometric behavior was observed when film morphology varied with film growth. Polyvinylferrocene films in 0.1*M* $TBABF_4$/acetonitrile were shown to be 15% thicker in the oxidized form than in the reduced form.

Polymer-modified electrodes are prepared by coating thin (100Å-2 μm) films of polymers on conductive substrates (1, 2). These polymers can be electronically conductive ones (*e.g.*, polypyrrole or polyaniline) or those that contain electroactive centers (*e.g.*, polyvinylferrocene or doped Nafion).

The electrochemical investigation and characterization of electron and mass-transport processes in polymer-coated electrodes has suffered from the lack of a simple and accurate technique for the determination of the polymer film thickness, *d*. Although the thickness of films in solution can be estimated from mechanical stylus profilometer (*e.g.*, Dektak) measurements of dry film thicknesses or from integrated voltammetric currents and assumed densities, uncertainties in the estimated film density, swelling factors, coulometric efficiency for film deposition, and redox processes lead to a low degree of

*Electrochemical Society Active Member.

confidence in the values of d obtained. Recently, *in situ* profilometer measurements of the change in thickness upon reduction of a film have been reported (3). The development of a generally applicable optical technique to determine d would be desirable, since optical methods are inherently precise and often suitable for measurements *in situ*.

Of the optical methods available for making thin film measurements, perhaps the most attractive for this purpose is ellipsometry (4). It has several advantages over other optical techniques: (*i*) it has already been successfully applied in the study of passivating and adsorbed layers in various electrochemical systems (4-8) [*e.g.*, in the anodic growth of passivating oxide layers on metal electrodes (8)], as well as in the study of electroinactive polymers on semiconductors (9, 10); (*ii*) it does not require a transparent electrode, only an optically smooth electrode surface; (*iii*) it does not require the determination of absolute light intensities; and (*iv*) it can be used to determine the thicknesses of layers much less than the wavelength of visible light. Although ellipsometry has been applied to the study of a wide variety of surfaces under various experimental conditions, it has not been used to characterize polymer-modified electrodes. In this paper, we describe *in situ* ellipsometric measurements on a series of polymer-modified electrodes and gauge its utility and limitations for several types of conductive and electroactive polymer coatings.

Experimental

Instrumentation.—Ellipsometry measurements were obtained on a modified O. C. Rudolph and Sons, Incorporated, Model 437 research ellipsometer [PSCA optical arrangement (4)]. The source was a tungsten/iodine lamp, and wavelengths suitable for the quarter-wave plates available were isolated with interference bandpass filters. Detection was accomplished with a Hamamatsu R928 photomultiplier tube by passing the output photocurrent through a variable resistance box and measuring the resulting voltage with a digital voltmeter. Measurements were made for a range of compensator/analyzer settings around the null-point, which, by interpolation, could generally be determined to within 0.3° for either the compensator or analyzer azimuth. Inaccuracies due to optical components' nonideality and improper alignment were somewhat larger than this and were functions of the reflection polarizations. These errors could be largely eliminated by averaging the calculated optical parameters obtained with the two unique compensator positions which allowed the reflection to be extinguished (*i.e.*, fast axis along the major or minor ellipse of polarization). The procedure was generally not applied, however, because it required doubling of an already lengthy (approximately 10 min per point) data collection time and because the corrections had little effect on the estimated film thickness or morphology.

The cell used during the ellipsometry measurements is shown in Fig. 1. The cell top and base were constructed of either stainless steel or Plexiglas. The window openings are 1/8 in. holes positioned so that incident light can strike the electrode at 45°, 60°, or 75° angles. The cell tops were machined so that glass windows could be cemented in place perpendicular to the direction of propagation of the incident or reflected radiation. Glass or Plexiglas side plates were also cemented in place. The electrode was a 0.5 cm diam piece of glassy carbon attached with conductive epoxy cement to the end of a brass rod. This assembly was inserted into a heat-softened Teflon tube which was cooled and threaded. The electrode surface was polished with increasingly finer diamond paste and alumina, ending with 0.05 μm alumina. Electrodes were sonicated for at least 10 min in deionized water before use.

Materials.—Acetonitrile, MeCN (Fisher Scientific), was dried with 0.4 nm molecular sieves (M-512, Fisher Scientific). Tetrabutylammonium tetrafluoroborate, $TBABF_4$ (Southwestern Analytical Chemicals), and methylene

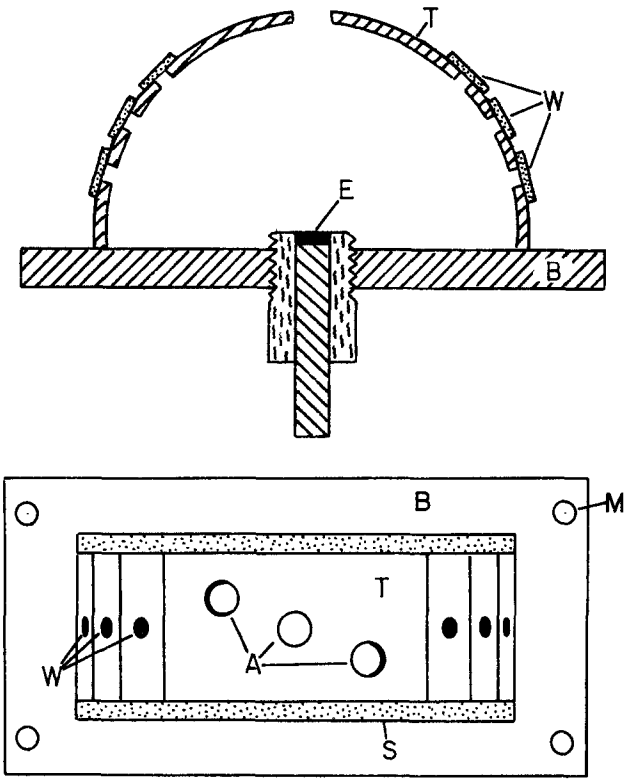

Fig. 1. Ellipsometer cell. Indicated are the cell top (T) and base (B), windows (W), sides (S), electrode (E), and mounting hole (M) and access ports (A) through which pass the counter and reference electrodes.

chloride, CH_2Cl_2 (Fisher Scientific), were used as received. Aniline (MCB) was distilled once from calcium hydride under nitrogen. Bipyrazine, bpz, was used as received from Professor A. B. P. Lever (York University). Polyvinylferrocene, PVF, was prepared and characterized (MW = 15,700; degree of polymerization = 74) by T. W. Smith *et al.* (11). Copolymers of vinylferrocene and vinylcyclopentadienylmanganeses tricarbonyl, VF-VCM (80/20 and 22/78 mole percent [m/o] ratio), were prepared and characterized by Dr. C. U. Pittman, Jr., *et al.* (12).

Film deposition.—Bipyrazine was electrochemically polymerized onto glassy carbon (13) from 3 mM bpz/10% aqueous H_2SO_4 by cycling the electrode potential at 500 mV/s between 1.5 and 2.1V *vs.* a saturated calomel electrode (SCE). The potential for bipyrazine oxidation is close to that of water, so a clearly defined wave for bpz oxidation cannot be resolved in the cyclic voltammograms and bpz oxidation currents cannot be monitored. Ellipsometry measurements were made both on the dry electrode and *in situ* with the potential held at 1.5V *vs.* SCE. For the former experiments, the polymer was deposited outside of the ellipsometer cell and the electrode was rinsed with deionized water and dried with a stream of nitrogen gas.

Polyaniline films (14) were deposited by electrochemical oxidation of aniline from 100 mM aniline/1M aqueous H_2SO_4 solutions either potentiostatically (at 0.8V *vs.* SCE) or by cycling the applied potential between −0.2 and 0.8V *vs.* SCE. Ellipsometry measurements were made *in situ* with the potential held at −0.2V *vs.* SCE.

Polyvinylferrocene and the VF-VCM copolymers were anodically precipitated from 0.1M $TBABF_4/CH_2Cl_2$ containing 0.2 mg of polymer per ml of solution (15). Deposition potentials were generally 200 mV positive of the PVF redox potential, *i.e.*, about 0.7V *vs.* a silver wire reference electrode. Ellipsometry measurements were made with the electrode in either the deposition solution or a 0.1M $TBABF_4$/MeCN solution. For the latter method, optically higher quality films were obtained by dipping the film-coated electrode once into each of the following rinses: 0.1M $TBABF_4$/MeCN, 0.05M $TBABF_4$/MeCN, and neat MeCN.

Analysis.—The optical constants of the polymer films generated by the above techniques were obtained by simulating a series of ellipsometry curves (ψ *vs.* Δ) and visually choosing the best fit of the experimental ψ and Δ. In general, there are four constants (the refractive indexes of the solution or gas phase contacting the film, N_0, and of the substrate, N_2; the angle of incidence, ϕ; the wavelength, λ), one variable (thickness, d), and one parameter (film refractive index, N_1) necessary in generating a particular curve. In all cases, N_0 was determined independently with an Abbe refractometer and ϕ and λ set to values appropriate to the experiment. The assignment of N_2 was made by determining ψ and Δ for the bare electrode and calculating a bulk refractive index. For this study, it was assumed that displacement of any adsorbate or chemical modification of the electrode surface upon polymer deposition caused no significant change in N_2. Ignoring the correction procedure described above did not have a significant effect on the choice of N_1 (and, therefore, the calculated d), but did lead to a small, finite deviation of the experimental data from ideal behavior for films of high optical quality. For the films described below as being nonideal (*i.e.*, inhomogeneous or nonuniform), this instrumental error can be considered insignificant.

Results

Polybipyrazine.—Electrochemical formation and deposition of a polymer film on an electrode is especially convenient because the ellipsometric parameters can be determined as the film grows. For a film of uniform density, refractive index, and thickness (d), the expected ψ *vs.* Δ plot would be periodic with one complete cycle occurring when d equals about one-half the wavelength of the incident light wave. Typical data obtained for the *in situ* deposition of polybipyrazine are shown in Fig. 2. The refractive index of the deposition solution was 1.387, and the calculated N_2 for the glassy carbon electrode immersed in that solution was 1.82-*i*0.67. The experimental data shown in Fig. 2 do not follow the expected ideal behavior for a nonabsorbing film because the points are not exactly periodic as the film thickness approaches 250 nm. The particular values of N_1 for the simulations in Fig. 2 were chosen by fixing the real part and determining the imaginary part that provided the best fit of the data in the first cycle of the polarization curve. It was difficult to determine the exact precision in N_1 (and d), but based on a series of simulations that provide a reasonably good fit to the experimental data, d is probably known to within ± 10% for the thinnest (<50 nm) films and within ± 3% for the thicker films. The two best fits, for N_1 = 1.63-*i*0.022 and 1.64-*i*0.017, are those shown in Fig. 2. There is an obvious deviation of the experimental from the simulated curves for the thickest films. Such behavior is characteristic of a nonuniform or variable thickness film (see "Discussion" section), and in general the

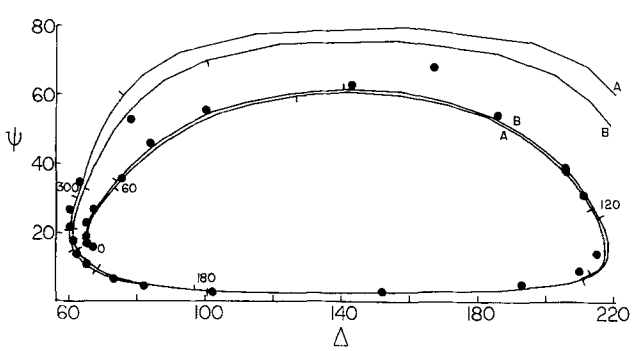

Fig. 2. *In situ* experimental (●) and simulated (———) data for reduced (1.5V *vs.* SCE) polybipyrazine deposited from 3 mM bipyrazine in 10% aqueous H_2SO_4 (N_0 = 1.387). The simulations consist of line segments connecting calculated points for films in 3 nm increments. The complex refractive indexes are (A) 1.63-*i*0.022 and (B) 1.64-*i*0.017. Indicated *d* are in nm.

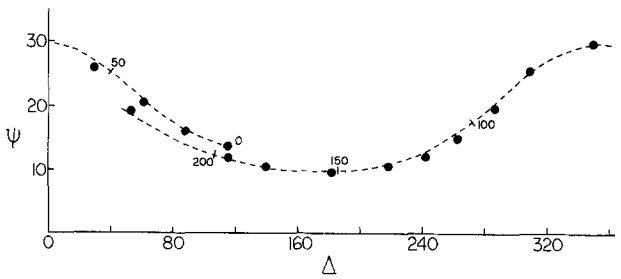

Fig. 3. Experimental (●) and simulated (– – –) data for dry polybipyrazine films. The simulation is for N_1 = 1.64-*i*0.035. Indicated *d* are in nm.

bipyrazine films grown in the ellipsometer cell were often visibly nonuniform. Since similar data for thicker polymer films is consistent with an imaginary component of N_1 of about 0.025, curve A (N_1 = 1.63-*i*0.022) probably represents the best fit of the data in Fig. 2. The results for dry polybipyrazine appear in Fig. 3. The dotted line demonstrates the excellent fit of the data to the simulated curve for N_1 = 1.64-*i*0.035 (N_2 = 1.84-*i*0.70).

Figure 4 contains plots of estimated thickness of wet and dry polybipyrazine layers as a function of number of deposition cycles. In general, it was difficult to control the deposition rate of these films from day to day. The bipyrazine oxidation wave is buried under that of the solvent, so small relative changes in deposition potential (due, perhaps, to electrode pretreatment) or in the reference electrode potential could lead to significant changes in deposition rate. Measurements on a particular film in both the wet and dry states indicate that polybipyrazine exhibits very little swelling, so that most of the difference in the observed deposition rates in Fig. 4 can be attributed to variations in experimental parameters or deposition technique. Figure 4 contains two notable features: a wide linear growth region and an initial stage of apparently more rapid deposition. The significance of these characteristics is discussed below.

Polyaniline.—All attempts to obtain ideal plots of ψ *vs.* Δ for the polyaniline deposition were unsuccessful. Figure 5 contains the best set of results for the reduced polymer which was obtained for films deposited by cycling the working electrode potential between −0.2 and 0.8V *vs.* SCE. A good fit, dashed line, of the early data (to a half-cycle) was obtained for N_0 = 1.346 and N_1 = 1.60. The spi-

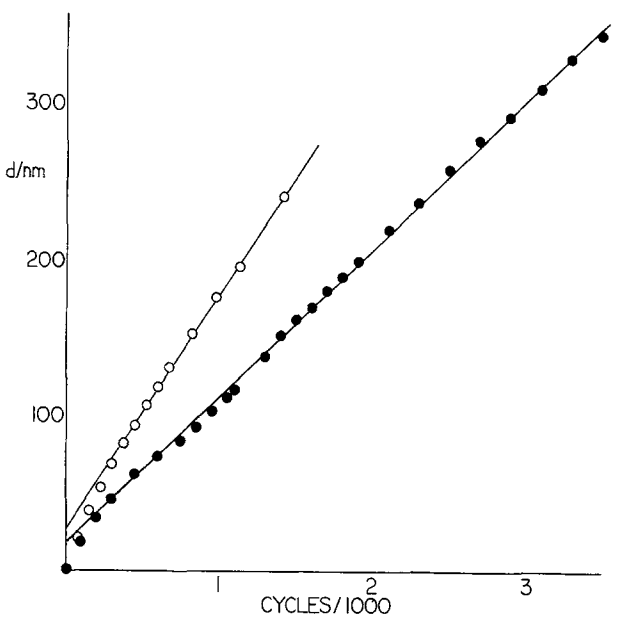

Fig. 4. Growth curves for reduced *in situ* (●) and dry (○) polybipyrazine films. Films were grown under different conditions (see text).

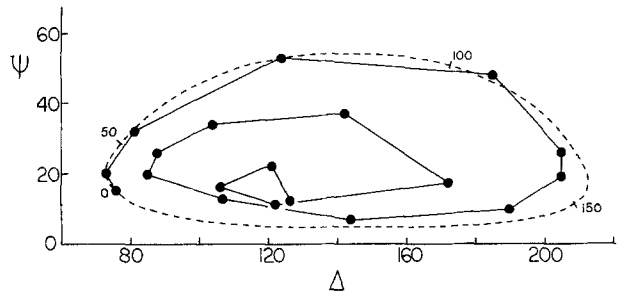

Fig. 5. Reduced (−0.2V vs. SCE) polyaniline which was deposited from 100 mM solutions in 1M H_2SO_4 by cycling the electrode potential between −0.2 and 0.8V vs. SCE. The curve (– – –) is that predicted for N_1 = 1.61. Indicated d are in nm.

raling inward of the ψ vs. Δ data after a half-cycle was accompanied by a marked decrease in the absolute reflectivity and the increasingly hazy appearance of the electrode surface. Potentiostatically growing the polymer produced a coating with obviously poorer optical properties.

Polyvinylferrocene and VF-VCM copolymers.—Attempts to monitor film deposition of PVF in 0.1*M* $TBABF_4/CH_2Cl_2$ solution were unsuccessful. Although a steady increase of oxidized polymer on the electrode surface could be verified by cyclic voltammetry and typical surface waves were observed, there were only very small changes in the reflection polarization of 546 nm light. Oxidation for several hours resulted in the appearance of a blue-green flocculent material on the electrode surface and a decrease in absolute reflectivity, but little change in the reflection polarization. These results suggest that PVF deposits as a highly solvated layer on the electrode surface.

Ellipsometric measurements on films deposited in 0.1*M* $TBABF_4/CH_2Cl_2$ and transferred with rinsing to 0.1*M* $TBABF_4$/MeCN for measurement produced plots of ψ vs. Δ from which d could be determined. Rapid growth (5-10 nm/min) was apparent from both electrochemical and optical measurements. Figure 6 contains results for an accumulative deposition in which the electrode was repeatedly transferred between deposition and observation solutions. Starting with the bare electrode and proceeding around the dashed curves, each point represents the reflection polarization observed for a film grown thicker between points. The circular and triangular points correspond to the film in the oxidized and reduced (neutral) states, respectively. Simulations are shown by solid lines connecting points calculated for 10 nm film thickness increments. Each simulated curve represents a fit of the first five data points for each oxidation state with N_0 = 1.347 (measured) and N_2 = 1.81-*i*0.66 (calculated). These data indicate that the oxidized form of the polymer film has a lower refractive index (1.48 *vs.* 1.53) and is 15% thicker than the reduced form (Fig. 7). The experimental ψ *vs.* Δ plots in Fig. 6 are clearly aperiodic and spiral inward in a fashion similar to that of polyaniline.

Figure 8 is a plot of measured thickness *vs.* integrated reduction current for a reduced PVF film that displayed good optical properties up to a thickness of 325 nm. This film was grown and studied in the same manner as the film discussed above, except that it was not allowed to dry during the rinsing and transferring procedure. In addition to having reflection polarizations which were close to the ideal behavior for N_1 = 1.51, it exhibited, for a scan rate of 10 mV/s, thin-layer cyclic voltammetric waves from which integrated reduction currents were obtained. The plot is fairly linear, as would be expected for a film depositing with uniform density and electroactivity.

Unlike the homopolymer, the deposition of the copolymers could be monitored directly in the deposition solution. Very slow deposition (several hours being required to obtain the data shown) of the 22% ferrocene VF-VCM yielded a reasonable plot of ψ *vs.* Δ to about 150 nm (Fig. 9). The refractive index of the film was about 1.52, and N_0 was 1.424. Also shown in Fig. 9 is a plot of thickness *vs.* integrated reduction current. The deposition of optically detectable polymer film becomes very inefficient at a thickness of about 150 nm. The surface became noticeably hazy when growth of thicker films was attempted. A spiraling inward of the ellipsometry plot may be occurring, but scattering caused the loss of so much signal that additional data could not be obtained. If the electrodes were washed in acetonitrile, however, a partial restoration of surface reflectivity was observed, without removal of all of the polymer layer. Similar behavior was observed with 80%/22% VF-VCM.

Discussion

Polybipyrazine.—Of the films studied, polybipyrazine exhibited the best optical characteristics. The deviation of the experimental data in Fig. 2 from that expected for a single layer of refractive index 1.63-*i*0.022 is most likely due to a nonuniform film thickness across the electrode surface. Because of instrumental limitations, a relatively large area, 0.1 cm^2, or approximately 50%, of the electrode surface had to be included in any optical measurement. If this film is not passivating (as Fig. 4 suggests), nonuniform deposition due to, for example, edge effects, may

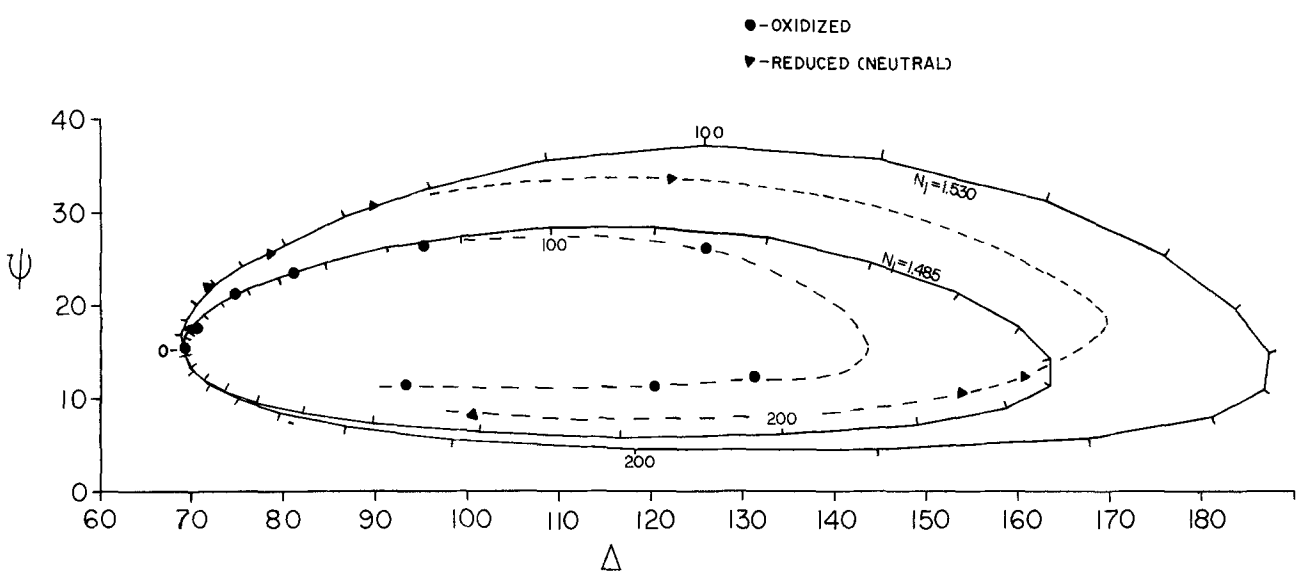

Fig. 6. Experimental and simulated polarizations for PVF films deposited from methylene chloride and transferred to acetonitrile. The simulations are the best fits of the first five points for each oxidation state. Tic marks are placed every 10 nm. The dashed lines are included only for clarity.

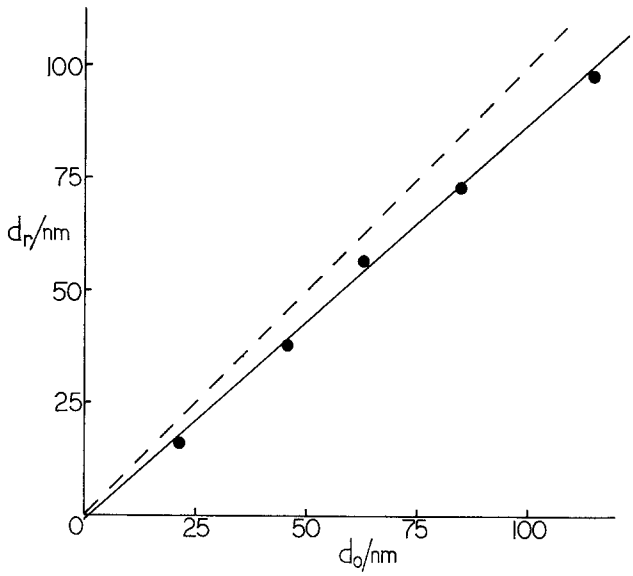

Fig. 7. Reduced (d_r) *vs.* oxidized (d_o) PVF polymer film thicknesses from data and simulations in Fig. 6.

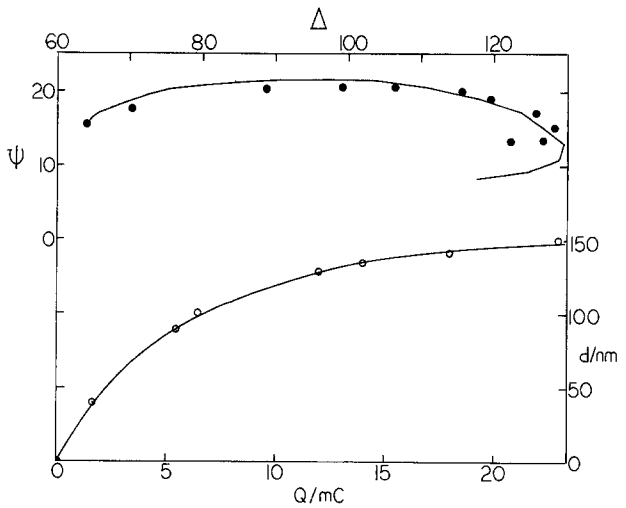

Fig. 9. Data for the *in situ* deposition of 22/78 PVF/VF-VCM in methylene chloride. The top curve represents an attemped fit with $N_1 = 1.52$. The bottom curve is a plot of estimated thickness *vs.* total deposition charge passed.

lead to a relative variation in film depth, d, which is independent of the effective mean thickness. The theoretical plots of ψ *vs.* Δ shown in Fig. 2 were made by drawing straight lines between calculated points every 3 nm; the effects of nonuniformity would be expected to be most apparent in the regions of these curves where both ψ and Δ are strongly dependent on thickness. In Fig. 2, this occurs when ψ is close to its maximum for a particular cycle. In this region, a spread of reflection polarizations (*i.e.*, depolarization) would lead to an observed ψ which is lower than expected for a uniform film. The effect is much more noticeable in the second cycle because the absolute variation in film thickness could be considerably greater (because the film is three times thicker) and, for absorbing films, the dependence of ψ and Δ on d is somewhat greater. Instrumental designs (14) which permit higher spatial resolution would be required to study thicker films, because this type of variability in d will eventually lead to depolarization sufficient to render thickness information unobtainable. Alternatively, the use of a profiling ellipsometer system (17) could provide coverage information for the entire electrode surface.

The data for the dry polybipyrazine film (Fig. 3) is interesting, because its refractive index is very similar to that of the wet film (*i.e.*, the real part of N_1 equal to 1.64 *vs.* 1.63 for the wet polymer). Since little swelling was observed between the wet and dry polymer, this behavior suggests either that solvent is mostly excluded from the reduced polymer layer, as might be expected for a neutral organic film, or that the air-dried film retained a significant amount of solvent. The former seems unlikely because rapid diffusion of hydroquinone through the reduced polymer has been observed (13).

Another interesting result of the polybipyrazine experiments is contained in Fig. 4. A plot of the ellipsometrically determined coating thickness *vs.* the number of deposition cycles clearly indicates that the polymer layer is not passivating toward continued deposition for layers of up to 325 nm. This implies that electron transport is rapid within the oxidized film (and the film is capable of oxidizing the monomer) and/or that mass transport of the monomer to the electrode surface (through the film) is not significantly limited by the presence of the polymer layer. These results are consistent with the electrochemical findings (13). Although, taken alone, these ellipsometry data cannot be used to deduce the mechanism of film deposition for polybipyrazine, they do show that ellipsometry may provide supportive evidence about the nature of the film in such an investigation. For example, the initial deposition rate for films <70 nm thick is twice that of the limiting rate (see Fig. 4).

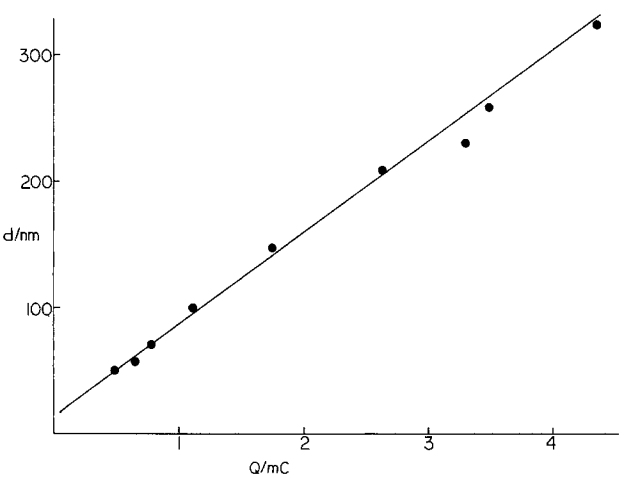

Fig. 8. Thickness *vs.* integrated reduction currents for PVF

Polyaniline.—Although ellipsometry does not yield useful thickness measurements for $d > 150$ nm, the polyaniline results are significant in that they demonstrate the sensitivity of the ellipsometric technique to film morphology. For the data presented in Fig. 5, reasonably precise film thicknesses can be obtained during the early stages of film growth. Optically, this film behaves well to about 150 nm, as is evident by the good fit of the data to a curve for $N_1 = 1.60$ and by the fact that macroscopic examination of the electrode surface showed a highly reflective surface. For thicker films, the optical characteristics of the polyaniline layer changed, as is evident from the inward spiral of the ellipsometry data. Simulations using various combinations of real and imaginary components for N_1 confirm that the unusual behavior of the measured ψ and Δ in Fig. 5 cannot be described by ellipsometry theory for homogeneous films, so effects of inhomogeneity and/or surface roughness must be considered. The theory for inhomogeneous coatings has been developed (4), but in general, closed-formed solutions for the ellipsometry equation cannot be obtained, even if a functional description of the depth-dependent refractive index is available (18). Calculations may be made if the film is approximated by a series of discrete homogeneous layers. If the refractive index of these layers is assumed to decrease with distance from the substrate/film interface, the simulated curves spiral inward in a fashion similar to the observed polyaniline curves. However, optical and electron microscopy (not shown) indicate that

the deposition of a relatively dense polymer layer up to 150 nm is followed by the growth of loosely packed fiberlike structures which have diameters of about 200 nm. Fibrous structures of this size cause roughness effects that would preclude the use of a multiple layer (microscopic) approach to the simulation of the ellipsometry data and would force the use of theories for the treatment of gross roughness (19). Additional data, such as multiple angle measurements, will be required to determine whether a particular model is valid.

The optical properties of the polyaniline films depend on the deposition technique. The data in Fig. 5 are for a film deposited by cycling the electrode potential as described in the experimental section, while potentiostatically-grown films exhibited much poorer optical characteristics. The fiberlike structures found in the thicker films are clearly electronically conductive, since microscopic examination of the film during oxidation and reduction shows rapid changes in the color of the fibers during electrochemical cycling. Growth of these fibers may be analogous to the growth of needlelike crystals of conductive tetrathiafulvalenium bromide in Nafion films (20, 21). These results suggest a changing mechanism for film deposition. The initially deposited film is much more dense, because the possibility of monomer oxidation directly at the electrode is high. As it becomes increasingly difficult for monomer to reach the electrode surface, oxidation at the termini of the conductive aniline chains becomes the dominant Faradaic process, leading to fiber production. Attempts have been made to improve the homogeneity of the aniline polymers by using different potential pulse or controlled current deposition programs, but little improvement in the optical characteristics of the films above 150 nm has been realized.

Polyvinylferrocene and VF-VCM copolymers.—PVF films produced by prolonged oxidation in methylene chloride could not be detected *in situ*, indicating that PVF deposits as a very diffuse, highly solvated layer. A film was obviously being formed, because the blue-green flocculent material was observed on the electrode, and large cyclic voltammetric surface-waves resulted when the applied potential was scanned negatively. The lack of change in the reflection polarization indicates, however, that the oxidized film had a refractive index that was not significantly different than that of the deposition solution.

The copolymers deposited more densely than PVF in methylene chloride, and it was possible to monitor their growth *in situ* up to thicknesses of 150 nm (see Fig. 9). At this point, deposition either effectively ceased or the density of newly deposited film became too low to be optically detected. These films grew much more slowly (about 50 nm/h) than PVF, which may have enhanced their ability to pack more densely, thus permitting one to monitor their growth in the deposition solution. The limiting factor in measuring the thickness of these films appears to be their inherent nature to grow inhomogeneously.

Films grown in methylene chloride and directly transferred into acetonitrile without rinsing resulted in ψ *vs.* Δ curves which spiraled quickly inward and cyclic voltammetric waves that showed diffusional tailing. This kind of ellipsometric behavior would be expected, as discussed above, of a film whose refractive index (and, therefore, density) decreases with distance from the electrode or whose surface is becoming increasingly rough. A precise description of the inhomogeneity would be important to know if one expects to model the electrochemical behavior of this redox polymer successfully.

The sensitivity of ellipsometry to roughness and/or inhomogeneity dictated that procedures be found to improve the quality of PVF films. Variability of film quality was a persistent problem, and ellipsometric characterization proved a useful diagnostic tool for ascertaining if a film was depositing uniformly. Nonideal growth could be observed early, long before the appearance of any light scattering or tailing cyclic voltammetric waves. Since PVF is slightly soluble in neat MeCN, but insoluble in 0.1*M* $TBABF_4$/MeCN, the films were rinsed as described in the "Deposition" section. The films were ellipsometrically observed to become thinner by this procedure. MeCN probably dissolves any loosely-bound outer layer and also solvates the film, thus improving its homogeneity. Films of improved optical and electrochemical quality could be grown to 300 nm by rinsing the electrode between depositions in this fashion, and ellipsometry curves (not shown) spiraled inward less dramatically. High surface reflectivity could generally be restored by this procedure with minimal concurrent loss of polymer.

Although homogeneous and uniform films were difficult to grow, Fig. 7 and 8 indicate that useful information could be obtained over a limited range of d. Figure 7 is especially interesting in that it represents the first reliable measurement of an oxidation/reduction swelling coefficient for an electroactive polymer. The observed decrease in film refractive index and increase in thickness that occurs upon oxidation of the polymer suggests that PVF is swelled by the uptake of counterions and attendant solvent molecules. The measured swelling coefficient (determined from the slope of the line in Fig. 7) is 1.15. Although allowance for film absorptivity has not been made, it is believed that this would be small, because the films in Fig. 7 are rather thin, and measurements on thicker (though somewhat inhomogeneous) films do not indicate that absorption is a problem.

The data in Fig. 8 allow comparison to be made between PVF film thicknesses determined ellipsometrically and by a nonoptical technique. The slope of the line in Fig. 8 provides a thickness/charge relationship given by

$$d = (1.9 \times 10^{-3}\ \mathrm{cm^3 C^{-1}})Q/A \qquad [1]$$

where d is the thickness, in cm, Q is the charge passed to reduce the totally oxidized film, in coulombs, and A is the electrode area, in cm^2. This finding is consistent with previously published results (22) for thicker PVF polymer films. The concentration of electroactive redox centers, C, is approximated (assuming $n = 1$) by

$$C = Q/dA\mathbf{F} \qquad [2]$$

where $\mathbf{F}$ is Faraday's constant. From the experimental expression for d, one obtains

$$C = (\mathbf{F} \times 1.9 \times 10^{-3}\ \mathrm{cm^3 C^{-1}})^{-1} \simeq 5M \qquad [3]$$

which is consistent with a reasonably densely packed array (~1.1 g/cm^3) of ferrocene moieties.

Conclusion

It has been shown that the ellipsometric technique can be applied successfully to the *in situ* study of electroactive polymer-modified electrodes. Data have been presented on three classes of electroactive polymer materials.

The conductive polymer, polyaniline, exhibits a very inhomogeneous morphology and at best displays ideal optical properties only up to 150 nm. Thickness and structural information for polyaniline films with a thickness greater than this will require multiple angle studies in order to apply microscopic or gross roughness theories to this system. Ellipsometry may prove to be useful in attempts to monitor and control the morphology of conductive films.

In situ measurements for the electroprecipitated redox polymers (PVF and the copolymers) have proven to be capable of providing redox site concentrations (necessary for electrochemical studies), as well as information on morphological changes that occur upon oxidation or reduction of these films. Detailed ellipsometric studies will eventually assist in the understanding of the mechanisms of charge transport in this important class of compounds.

Electropolymerized bipyrazine yielded the best films for the ellipsometric determination of thickness. Al-

though instrumental and sample problems limited our ability to make precise measurements for thicknesses beyond about 400 nm, analysis of much thicker layers is well within reach.

As a general tool for the study of polymer modified electrodes, ellipsometry will eventually be limited by effects of gross roughness and film nonuniformity. Implementation of improved cell designs and more complex theoretical considerations may improve its utility in this field. Data acquisition with an automatic ellipsometer and at multiple wavelengths should also aid in the elucidation of the structure and behavior of polymer films on electrodes.

Acknowledgments

The authors wish to thank Dr. Frank Fan, Dr. Pushpito Ghosh, Dr. Johna Leddy, and Dr. Alex McDonald for their helpful assistance and comments. The support of this work by the National Science Foundation (CHE84-02135) and the Robert A. Welch Foundation (F-079) is gratefully acknowledged.

Manuscript submitted May 14, 1984; revised manuscript received Sept. 24, 1984.

REFERENCES

1. R. W. Murray, in "Electroanalytical Chemistry," A. J. Bard, Editor, pp. 191-368, Vol. 13, Marcel Dekker, New York (1984).
2. W. J. Albery and A. R. Hillman, *Chem. Soc. Annu. Rep. C.*, 377 (1981).
3. T. Lewis, H. S. White, and M. Wrighton, Private communication.
4. R. M. A. Azzam and N. M. Bashara, in "Ellipsometry and Polarized Light," pp. 269-363, North-Holland Publishing Co., New York (1977).
5. W. Paik, M. A. Genshaw, and J. O'M. Bockris, *J. Phys. Chem.*, **74**, 4266 (1970).
6. E. Yeager, *Surf. Sci.*, **101**, 1 (1980).
7. J. Kruger, in "Advances in Electrochemistry and Electrochemical Engineering," P. Delahay and C. W. Tobias, Editors, pp. 227-280, Vol. 9, John Wiley and Sons, New York (1973).
8. Several recent examples include: W. Kozlowski and A. Szklarska-Smialowska, *This Journal*, **131**, 723 (1984); J. L. Ord, *ibid.*, **129**, 767 (1982); C.-T. Chen and B. D. Cahan, *ibid.*, **128**, 17 (1982); S. Silverman, G. Cragnolino, and D. D. MacDonald, *ibid.*, **129**, 2419 (1982); T. Ohtsuka and N. Sato, *ibid.*, **128**, 2522 (1981).
9. R. Scheps, *ibid.*, **129**, 2273 (1982).
10. R. Scheps, *ibid.*, **131**, 540 (1984).
11. T. W. Smith, J. E. Kuder, and D. Wychik, *J. Polym. Sci., Polym. Chem. Ed.*, **14**, 2433 (1976).
12. C. U. Pittman, Jr., G. V. Marlin, and T. D. Rounsefell, *Macromolecules*, **6(1)**, 1 (1973).
13. P. K. Ghosh and A. J. Bard, *This Journal*, In press.
14. A. F. Diaz and J. A. Logan, *J. Electroanal. Chem.*, **111**, 111 (1980).
15. A. Merz and A. J. Bard, *J. Am. Chem. Soc.*, **100**, 3222 (1978).
16. K. Sugimoto and S. Matsuda, *This Journal*, **130**, 2323 (1983).
17. M. Stenberg and H. Nygren, *Anal. Biochem.*, **127**, 183 (1982).
18. F. Abeles, in "Ellipsometry in the Measurement of Surfaces and Thin Films, Symposium Proceedings, Washington, 1963," E. Passaglia, R. R. Stromberg, and J. Kruger, Editors, pp. 41-58, National Bureau of Standards Miscellaneous Publication 256 (1964).
19. T. Smith, *J. Electroanal. Chem.*, **150**, 277 (1983).
20. T. P. Henning, H. S. White, and A. J. Bard, *J. Am. Chem. Soc.*, **103**, 3937 (1981).
21. T. P. Henning, H. S. White, and A. J. Bard, *ibid.*, **104**, 5862 (1982).
22. J. Leddy and A. J. Bard. *J. Electroanal. Chem.*, **153**, 223 (1983).

Electrocatalytic Oxidation of As(III)

II. Kinetic Studies at Pt Electrodes

Tim D. Cabelka,[1] Deborah S. Austin, and Dennis C. Johnson*

Department of Chemistry and Ames Laboratory,[2] Iowa State University, Ames, Iowa 50011

ABSTRACT

The empirical rate law for the electrocatalyzed oxidation of As(III) at a Pt RDE in acidic media was determined from potentiostatic measurements to be

$$k = k_o(t/t_o)^{-b} \exp\{-E/E_o\}$$

where t_o = 1.0s and E_o = 0.161V *vs.* SCE. For an electrode surface covered with less than the equivalent of a monolayer of PtO (*i.e.*, $Q_{ox}/Q_H < ca.\ 2$), b = 0.30, whereas for an extended oxide coverage (*i.e.*, $Q_{ox}/Q_H > 2$), b = 0.5. The coefficient k_o is independent of time (t) and electrode potential (E), but decreases as a function of the log of As(III) flux, *i.e.*, $\omega^{1/2}C^b_{As(III)}$. It is PtOH and not PtO that is the active agent for oxygen-atom transfer in the electrocatalytic mechanism. The finite rate of oxidation of As(III) observed for $Q_{ox}/Q_H >> 2$ is concluded to result from ·OH generated as the first step in the mechanism for continued oxide growth. It is concluded also that the generation of ·OH at a highly oxidized Pt surface occurs at a rate independent of applied potential.

A brief review of the electrochemical literature for As(III) was presented in part I of this work (1), together with our results of voltammetric studies at Pt rotating disk and ring-disk electrodes. The irreversible oxidation of $As(OH)_3$ at Pt electrodes in acidic media is electrocatalyzed dramatically by the anodic discharge of adsorbed ·OH (*i.e.*, PtOH) as the first step in (*i*) the production of surface oxide (*i.e.*, PtO) and (*ii*) the evolution of O_2(g) at an oxide-covered Pt surface. The rate of oxidation of As(III) is substantially lower at a surface covered by a well-developed layer of PtO with a rate constant (k), measured during the negative potential scan, which is independent of potential in the range $0.9 \leq E \leq 1.2$V *vs.* SCE. Hence, for a fixed quantity of surface oxide, the rate-determining step (rds) is not a charge-transfer step. The value of k measured at 1.0V on the negative potential scan for an oxide covered electrode decreases with increasing value of the anodic scan limit (E_a) for the preceding positive scan as described by

$$k = M \cdot \exp\{-E_a/E_o\} \quad [1]$$

where M and E_o are constants; the value of M was not studied for time dependence in part I (1). The charge corresponding to the total surface oxide (Q_{ox}) formed during a cyclic potential scan for $E_a \geq 1.0$V in the presence of As(III) is approximately the same as for the absence of As(III). Since Q_{ox} is a linear function of E_a (2), Eq. [1] can

*Electrochemical Society Active Member.

[1]Present address: Dow Chemical Company, Midland, Michigan 48640.

[2]Operated for the U.S. Department of Energy by Iowa State University under Contract no. W-7405-ENG-82.